

Supplementary Materials

Data on myeloid neoplasms patients (n=1804) derived from a collaboration between Cleveland Clinic Foundation and Munich Leukemia Laboratory and can be retrieved from: https://github.com/LucaGuarnera/Raw-data_Telomere-Project.git.

Supplementary Methods

Telomere content adjustment

To investigate the impact of karyotypic anomalies in TC, we adjusted our results by considering the number of chromosomes and the allelic burden of karyotype aneuploidies according to the following formula with the naive assumption that TC will correlate linearly with the number of chromosomes independently from the chromosome identity:

$$f(x) = \frac{\sum K_i * C_i}{\sum K_i * 46}$$

$$TC'_m = TC_m / f(m)$$

TC: telomere content.

K_i : Number of cells in which the type of karyotype was detected.

C_i : Number of chromosomes detected in the karyotype analysis.

In our analysis we decided not to account for copy number alterations (CNAs) which can be determined by WGS but most of the are intrachromosomal and work in both directions in terms of DNA content while not affecting the end of chromosomes. Similarly, they can be somatic as well as germ line.

Measurement of chromothriptic events

ShatterSeek¹ was used for identifying chromosomes harboring regions of chromothripsis. For this copy number and structural variation (SV) calls were generated from WGS as described previously². False positive SV calls were removed by an in-house filtering pipeline based on recurrence in a large reference panel. ShatterSeek was run using default settings and only calls with high levels of confidence were used for further analysis.

Telomere length estimation via PCR

To validate our WGS-based TC measurement we quantified an aliquot of samples via qPCR using ScienCell's Absolute Human Telomere Length Quantification qPCR Assay Kit (#8918). Primers

recognize and amplifies telomere length by comparing samples to the reference human genomic DNA (recognized by single copy reference primers). Reference DNA contains a 100 base pair telomere sequence located on chromosome 17 derived from human pulmonary alveolar epithelial cells. DNA was extracted as described above. PCR reactions contained DNA sample (0.01 µg/µL), telomere primer, 2x qPCR master mix, and nuclease-free water. The experiment was performed following manufacturer instructions. All reactions were performed in triplicate. Following the formula used to quantify TC:

$$\Delta Cq \text{ (TEL)} = Cq \text{ (TL, target sample)} - Cq \text{ (TL, reference sample)}$$

$$\Delta Cq \text{ (SCR)} = Cq \text{ (SCR, target sample)} - Cq \text{ (SCR, reference sample)}$$

$$\Delta\Delta Cq = \Delta Cq \text{ (TL)} - \Delta Cq \text{ (SCR)}$$

$$\text{TL (target samples)} = \text{Reference sample telomere length} \times 2^{-\Delta\Delta Cq}$$

Cq: cycle quantification

SCR: Single copy reference

TL: Telomere length

Statistical analysis

Quantitative variables were expressed as median, interquartile range, minimum and maximum. Qualitative variables were expressed as numbers and percentages. For all relevant comparisons, after testing for normal distribution, comparative analyses between two groups have been performed, as appropriate, by two-sided paired or unpaired Student's t-tests at 95% CI. In case of not normally distributed data, the Wilcoxon matched pairs signed rank test at 95% CI has been used. ANOVA, or Analysis of Variance, was used for comparison between >2 groups. Fisher test or Chi-square were used where appropriate. Multiple linear regression was used to analyze the relationship between a single dependent variable and several independent covariates. Ordinary least squares regression in multivariate setting was used where the significance of estimated coefficients are determined via t-test. Overall survival (OS) was defined as the time from diagnosis to last follow-up or death by any cause. OS was calculated using Kaplan–Meier estimator.

Univariate impact of baseline variables on OS was evaluated using the Log-Rank test. Multivariate impact of baseline variables was evaluated using a multivariate Cox-cause specific model.

All statistical tests were two-sided; a p-value < 0.05 was considered statistically significant. All analyses and data visualization were generated using the following statistical programs: IBM SPSS Statistics for Windows, Version 25.0. Armonk, NY: IBM Corp., Excel Microsoft Office 365 and GraphPad Prism (8.4.0).

Tables

Supplementary Table 1. Comparison of TC between non clonal controls and study cohort according to age.

Age range	Percentile	Non-malignant controls (TC)	Age range	Percentile	Non-malignant controls, n (%)	MN, n (%)	MDS, n (%)	AML, n (%)
20-29	25 th	653,0518	20-24	<25 TH	7 (87.5)	16 (94.1)	1 (100)	15 (93.7)
	75 th	715,8846		>75 TH	1 (12.5)	1 (5.9)	0	1 (6.2)
			25-29	<25 TH	8 (100)	20 (95.2)	1 (100)	19 (95)
			>75 TH	0	0	0	0	
30-39	25 th	322,2135	30-34	<25 TH	3 (60)	10 (40)	0	8 (47)
	75 th	603,9686		>75 TH	0	1 (4)	1 (25)	0
			35-39	<25 TH	2 (14.3)	10 (41.7)	2 (40)	10 (43.5)
			>75 TH	2 (14.3)	3 (12.5)	1 (20)	2 (8.7)	
40-49	25 th	314,9568	40-44	<25 TH	2 (16.7)	16 (35.6)	2 (20)	14 (40)
	75 th	570,2733		>75 TH	2 (16.7)	8 (17.8)	6 (60)	2 (5.7)
			45-49	<25 TH	1 (20)	22 (39.3)	4 (23.5)	18 (46.1)
			>75 TH	0	8 (14.3)	5 (29.4)	3 (7.7)	
50-59	25 th	373,2124	50-54	<25 TH	1 (12.5)	30 (46.1)	6 (26.1)	24 (57.1)
	75 th	590,5197		>75 TH	0	15 (23.1)	11 (47.8)	4 (9.5)
			55-59	<25 TH	3 (50)	43 (42.1)	14 (40)	29 (43.3)
			>75 TH	1 (16.7)	26 (25.5)	14 (40)	0	
60-69	25 th	344,9696	60-64	<25 TH	4 (40)	48 (40.7)	11 (19.3)	37 (60.6)
	75 th	545,8485		>75 TH	2 (20)	29 (24.6)	23 (40.3)	6 (9.8)
			65-69	<25 TH	0	73 (37)	26 (24.1)	47 (52.8)
			>75 TH	1 (12.5)	58 (29.4)	44 (40.7)	14 (15.7)	

Supplementary table 2. Telomere content and karyotype features in MN population.

Karyotype (n)	Mean TC	Median TC
Normal (645)	476.783	435.0882
Complex (132)	493.5511	391.4617
+8 (47)	462.715	385.8974
-7/del(7q) (27)	509.9361	473.2122
+13 (7)	416.9729	371.6058
inv(3)/t(3;3) (34)	510.7006	403.0274
t(6;9) (15)	327.4796	283.6136
t(8;21) (43)	329.3709	269.2388
inv(16) (46)	371.2676	337.3961
del(5q) (123)	545.1079	492.4535
del(20q) (14)	491.6656	490.0431
t(9;11) (37)	322.7982	302.6617
t(15;17) (49)	309.5283	290.773
-Y (44)	494.8383	510.0022
+1 (6)	433.9769	364.6835

Supplementary Table 3. Telomere content and gene mutations in MN cohort.

Mutation (n)	Mean TC	Median TC	Mutation (n)	Mean TC	Median TC
MN cohort (1432)	460.4653	405.693	<i>MPL</i> (12)	608.727	576.2221
<i>ASXL1</i> (211)	490.9895	438.8224	<i>NF1</i> (34)	444.173	340.9715
<i>ATM</i> (40)	405.5932	352.2996	<i>NPM1</i> (169)	357.3183	324.8324
<i>BCOR</i> (39)	485.7005	459.8681	<i>NRAS</i> (128)	415.2544	346.0577
<i>CALR</i> (9)	467.4743	483.3796	<i>PHF6</i> (35)	458.7436	435.9327
<i>CBL</i> (46)	416.1172	385.9623	<i>PTPN11</i> (45)	446.1825	365.9376
<i>CEBPA</i> (74)	486.6528	445.9839	<i>RAD21</i> (31)	406.6845	321.8893
<i>DNMT3A</i> (128)	437.3165	387.8943	<i>RUNX1</i> (133)	442.7191	389.7165
<i>ETV6</i> (27)	563.7419	531.4665	<i>SF3B1</i> (249)	506.8377	469.7206
<i>EZH2</i> (47)	459.7702	372.0034	<i>SMC3</i> (15)	375.0437	375.4041
<i>FLT3</i> (64)	342.1053	296.3229	<i>SRSF2</i> (172)	520.9906	472.8089
<i>GATA2</i> (35)	423.6785	413.8025	<i>STAG2</i> (75)	473.8821	435.3987
<i>GNAS</i> (8)	510.8518	490.1103	<i>TET2</i> (333)	480.3584	438.8224
<i>IDH1</i> (53)	423.2029	372.0202	<i>TP53</i> (146)	520.5212	439.8675
<i>IDH2</i> (81)	430.0042	387.776	<i>U2AF1</i> (66)	471.5033	422.2836
<i>JAK2</i> (29)	409.9237	397.5222	<i>WT1</i> (56)	350.9602	339.1066
<i>KRAS</i> (72)	362.2503	324.2885			

Supplementary Table 4. Multiple regression analysis for Telomere content including *TP53* mutation.

	p	β Coefficient	CI95%
Diagnosis (AML vs MDS)	0.163	-25.426	-61.182 – 10.331
Age	0.079	0.700	-0.082 - 1.482
Blast percentage	<0.0001	-1.223	-1.752 - -0.694
<i>TP53</i> Mutation	0.001	64.641	27.223 – 102.058
Karyotype (Abnormal vs Normal)	0.073	-21.163	-44.287 – 1.962

Supplementary Table 5. Multiple regression analysis for Telomere content accounting for CK.

	p	β Coefficient	CI95%
Blasts percentage	<0.001	-1.553	-1.890 - -1.215
Age	0.032	0.849	0.075-1.624
TP53 Mutation	0.017	56.037	10.160-101.914
CK	0.821	-5.485	-53.155-42.185

Supplementary table 6. Multiple regression analysis for Telomere content, including somatic mutations and karyotype abnormalities correlating with TC and potential biases due to chromothripsis events.

	p	β Coefficient	CI95%
Chromothripsis	<0.0001	72.729	50.136 – 95.341
Age	0.848	0.077	-0.712 – 0.866
Blast percentage	<0.0001	-1.005	-1.384 - -0.626
ASXL1 Mutation	0.312	16.250	-15.257 – 47.757
KRAS Mutation	0.001	-84.032	-132.957 - -35.107
NPM1 Mutation	<0.0001	-78.421	-115.889 - -40.952
NRAS Mutation	0.192	-24.826	-62.154 – 12.503
SRSF2 Mutation	0.005	49.145	15.242 – 83.084
TP53 Mutation	0.019	43.173	7.182 – 79.164
WT1 Mutation	0.033	-60.033	-115.055 - -5.011
t(15:17)	<0.0001	-119.788	-180.914 - -58.661
t(8:21)	<0.0001	-123.531	-185.930 - -61.133

Supplementary table 7. Multivariate analysis for overall survival in MN patients.

	p	HR	CI95%
Telomere content	0.218	1.000	1.000-1.001
Age	<0.0001	1.052	1.044-1.059
Blast percentage	<0.0001	1.018	1.016-1.021
TP53 Mutation	<0.0001	2.217	1.768-2.779
Gender (M vs F)	0.010	1.212	1.047-1.404
Abnormal Karyotype	0.003	1.259	1.082-1.465

Supplementary table 8. Multivariate analysis for overall survival in AML patients.

	p	HR	CI95%
Telomere content	0.078	1.000	1.000-1.001
Age	<0.0001	1.050	1.041-1.059
Blast percentage	<0.0001	1.008	1.004-1.012
TP53 Mutation	<0.0001	1.922	1.373-2.691
Gender (M vs F)	0.943	0.992	0.804-1.224
Abnormal Karyotype	0.069	1.234	0.984-1.547

Supplementary table 9. Multivariate analysis for overall survival in MDS patients.

	p	HR	CI95%
Telomere content	0.178	1	0.999-1
Age	<0.0001	1.049	1.036-1.061
Blast percentage	<0.0001	1.098	1.074-1.123
TP53 Mutation	<0.0001	2.285	1.646-3.172
Gender (M vs F)	0.002	1.386	1.125-1.707
Abnormal Karyotype	0.053	1.236	0.998-1.531

Supplementary table 10. List of genes involved in telomeres machinery screened.

Telomeres machinery genes			
<i>ACD</i>	<i>CTC1</i>	<i>DKC1</i>	<i>GAR1</i>
<i>NAF1</i>	<i>NHP2</i>	<i>NOP10</i>	<i>PARN</i>
<i>POT1</i>	<i>RAP1</i>	<i>RTEL1</i>	<i>TCAB1</i>
<i>TERC</i>	<i>TERF1</i>	<i>TERF2</i>	<i>TERT</i>
<i>TIN2</i>	<i>TINF2</i>	<i>TPP1</i>	<i>WRAP53</i>
<i>ZCCHC8</i>			

Supplementary table 11. List of variants identified in MN patients' population.

Gene	Genomic position	Ref	Alt	VAF	Pathogenicity
<i>ATRX</i>	76764089	G	A	0.42	LP
<i>ATRX</i>	76814312	C	G	0.7027	LP
<i>CTC1</i>	8133222	CAG	C	0.4545	P
<i>CTC1</i>	8138605	T	G	0.5106	LP
<i>CTC1</i>	8139541	GGACT	G	0.4643	LP
<i>CTC1</i>	8146468	T	G	0.4855	LP
<i>NAF1</i>	164058403	C	T	0.5	P ^ε
<i>NHP2</i>	177580563	T	A	0.4824	LP
<i>PARN</i>	14698072	A	AT	0.4364	P
<i>POT1</i>	124482952	G	GA	0.4776	P
<i>TERF1</i>	73951437	C	T	0.4833	LP
<i>TERT</i>	1271247	G	A	0.4599	VUS [†]
<i>TERT</i>	1280415	TC	T	0.5028	LP
<i>TERT_p</i>	1295228	G	A	0.365854	LP
<i>TERT_p</i>	1295228	G	A	0.467532	LP
<i>TERT_p</i>	1295250	G	A	0.4	P [‡]
<i>TPP1</i>	6636673	C	G	0.4674	P
<i>TPP1</i>	6637951	T	C	0.5	LP

Supplementary table 12. Patients included in C-Circle analysis.

Sample	<i>TP53</i>	TC	Telomere Class	Sample	<i>TP53</i>	TC	Telomere Class
UPN1	Mut	1043.65197	High	UPN23	Mut	1153.627743	High
UPN2	Mut	1345.190599	High	UPN24	Mut	1772.125595	High
UPN3	Mut	1018.121999	High	UPN25	Mut	1203.818244	High
UPN4	Mut	1018.68638	High	UPN26	Mut	2605.44884	High
UPN5	Mut	1056.247321	High	UPN27	Mut	1899.806706	High
UPN6	Mut	1282.613029	High	UPN28	Mut	1041.644114	High
UPN7	WT	1076.326501	High	UPN29	WT	1020.170139	High
UPN8	WT	1346.094469	High	UPN30	WT	1578.081978	High
UPN9	WT	1090.912322	High	UPN31	WT	1302.89036	High
UPN10	Mut	210.481559	Low	UPN32	Mut	272.404285	Low
UPN11	Mut	274.760884	Low	UPN33	Mut	123.815187	Low
UPN12	Mut	225.373816	Low	UPN34	Mut	216.238463	Low
UPN13	Mut	212.925231	Low	UPN35	Mut	215.210905	Low
UPN14	Mut	263.169937	Low	UPN36	Mut	242.964704	Low
UPN15	WT	145.323996	Low	UPN37	WT	287.719182	Low
UPN16	WT	153.26857	Low	UPN38	WT	158.136741	Low
UPN17	WT	156.239165	Low	UPN39	WT	147.44443	Low
UPN18	HS	747.061652	Normal	UPN40	HS	619.5652	Normal
UPN19	HS	669.147802	Normal	UPN41	HS	523.655962	Normal
UPN20	HS	519.049394	Normal	UPN42	HS	707.230111	Normal
UPN21	HS	611.588775	Normal	UPN43	HS	666.8728	Normal
UPN22	HS	624.004045	Normal	UPN44	HS	447.7075	Normal

Supplementary table 13. Placement of samples in the gel (UPN1-22).

	No Pol	Pol	No Pol	Pol	No Pol	Pol
	1	2	3	4	5	6
A	SKNBE2	SKNBE2	UPN7	UPN7	UPN15	UPN15
B	CHLA90	CHLA90	UPN8	UPN8	UPN16	UPN16
C	UPN1	UPN1	UPN9	UPN9	UPN17	UPN17
D	UPN2	UPN2	UPN10	UPN10	UPN18	UPN18
E	UPN3	UPN3	UPN11	UPN11	UPN19	UPN19
F	UPN4	UPN 4	UPN12	UPN12	UPN20	UPN20
G	UPN5	UPN5	UPN13	UPN13	UPN21	UPN21
H	UPN6	UPN6	UPN14	UPN14	UPN22	UPN22

Supplementary table 14. Numeric quantification of C-Circle analysis results (UPN1-22).

	Quantification					
	1	2	3	4	5	6
A	0	0	2954.125	2938.205	617.77	831.376
B	109.263	6568.912	1866.841	814.296	0	0
C	0	0	0	0	0	0
D	2643.376	1720.962	0	0	832.79	2193.598
E	0	0	0	0	873.012	436.134
F	2756.761	3382.669	0	0	1144.962	467.033
G	1883.69	2046.669	1754.79	797.79	770.598	893.669
H	1936.841	3348.841	1512.841	704.305	0	0

Supplementary table 15. Numeric quantification of C-Circle analysis results normalized to CHLA-90 positive control (UPN1-22).

	Relative to CHLA90					
	1	2	3	4	5	6
A	0.000	0.000	0.450	0.447	0.094	0.127
B	0.017	1.000	0.284	0.124	0.000	0.000
C	0.000	0.000	0.000	0.000	0.000	0.000
D	0.402	0.262	0.000	0.000	0.127	0.334
E	0.000	0.000	0.000	0.000	0.133	0.066
F	0.420	0.515	0.000	0.000	0.174	0.071
G	0.287	0.312	0.267	0.121	0.117	0.136
H	0.295	0.510	0.230	0.107	0.000	0.000

Supplementary table 16. Placement of samples in the gel (UPN23-44).

	No Pol	Pol	No Pol	Pol	No Pol	Pol
	1	2	3	4	5	6
A	SKNBE2	SKNBE2	UPN29	UPN29	UPN37	UPN37
B	CHLA90	CHLA90	UPN30	UPN30	UPN38	UPN38
C	UPN23	UPN23	UPN31	UPN31	UPN39	UPN39
D	UPN24	UPN24	UPN32	UPN32	UPN40	UPN40
E	UPN25	UPN25	UPN33	UPN33	UPN41	UPN41
F	UPN26	UPN26	UPN34	UPN34	UPN42	UPN42
G	UPN27	UPN27	UPN35	UPN35	UPN43	UPN43
H	UPN28	UPN28	UPN36	UPN36	UPN44	UPN44

Supplementary table 17. Numeric quantification of C-Circle analysis results (UPN23-44).

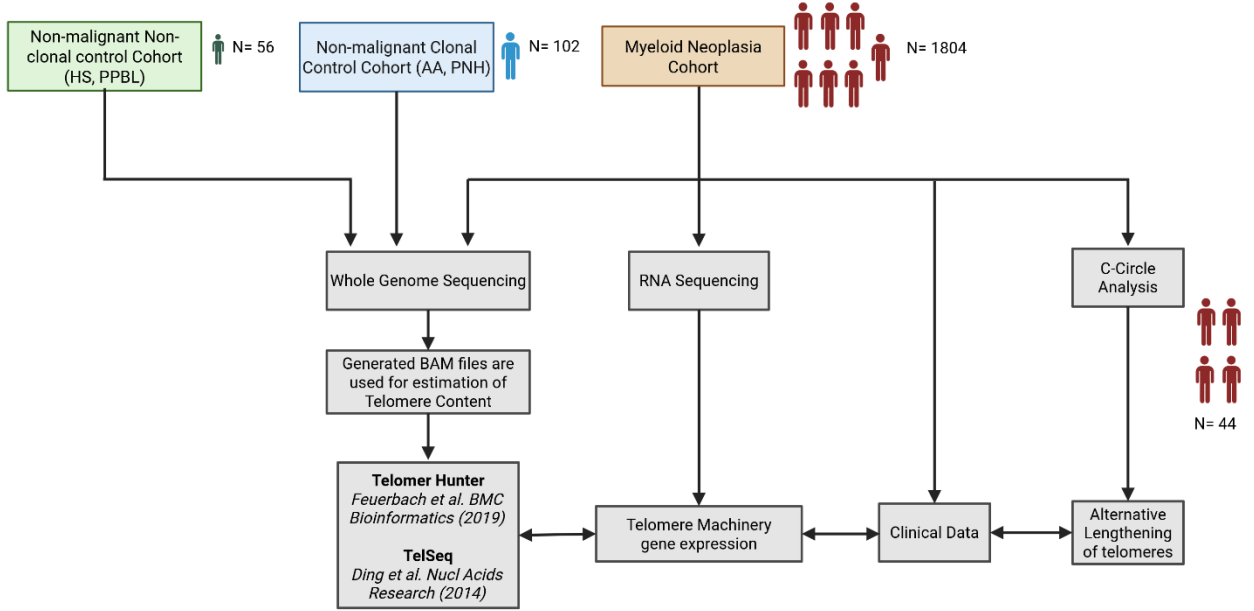
	Quantification					
	1	2	3	4	5	6
A			7857.104	6664.397		
B	90.213	5584.669	5999.912	3714.619		
C	6153.497	7915.912			2263.569	781.598
D	9276.69	6955.74	959.912	218.213	2371.497	663.497
E	11926.619	4835.983	477.012	1104.719	1453.841	432.205
F	4916.376	8213.79	768.154	1406.619	2682.569	994.426
G	827.255	739.497	660.134	645.79	3616.79	1572.054
H	2746.912	1077.79	674.79	681.74	1779.083	691.983

Supplementary table 18. Numeric quantification of C-Circle analysis results normalized to CHLA-90 positive control (UPN23-44).

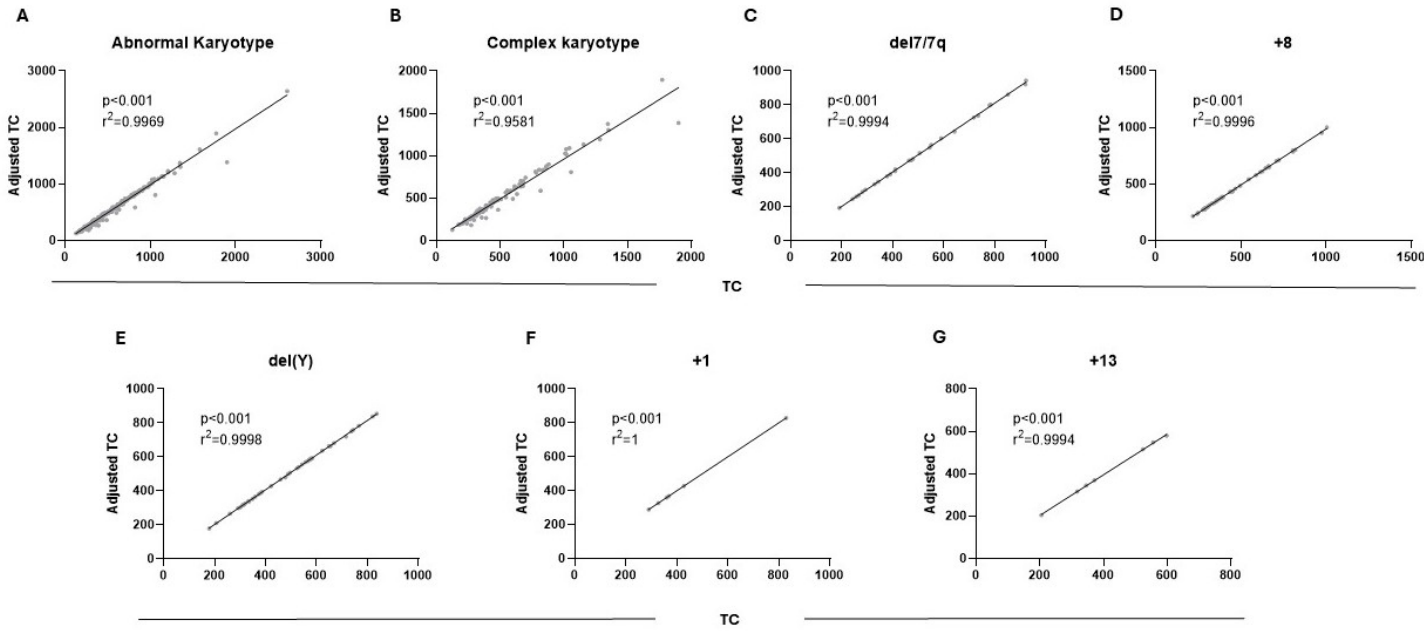
	Relative to CHLA90					
	1	2	3	4	5	6
A	0.000	0.000	1.407	1.193	0.000	0.000
B	0.016	1.000	1.074	0.665	0.000	0.000
C	1.102	1.417	0.000	0.000	0.405	0.140
D	1.661	1.246	0.172	0.039	0.425	0.119
E	2.136	0.866	0.085	0.198	0.260	0.077
F	0.880	1.471	0.138	0.252	0.480	0.178
G	0.148	0.132	0.118	0.116	0.648	0.281
H	0.492	0.193	0.121	0.122	0.319	0.124

Figures

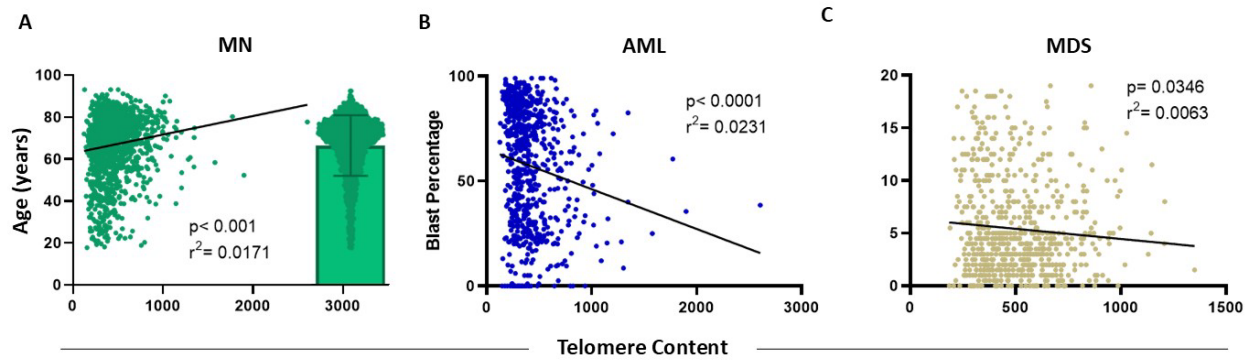
Supplementary figure 1. Study design.



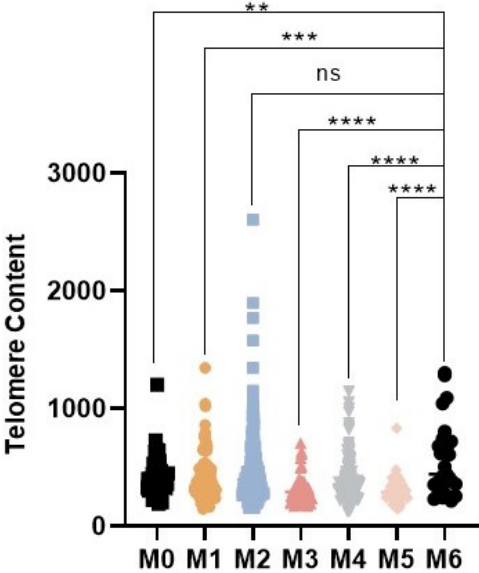
Supplementary figure 2. Impact of aneuploidy in TC.



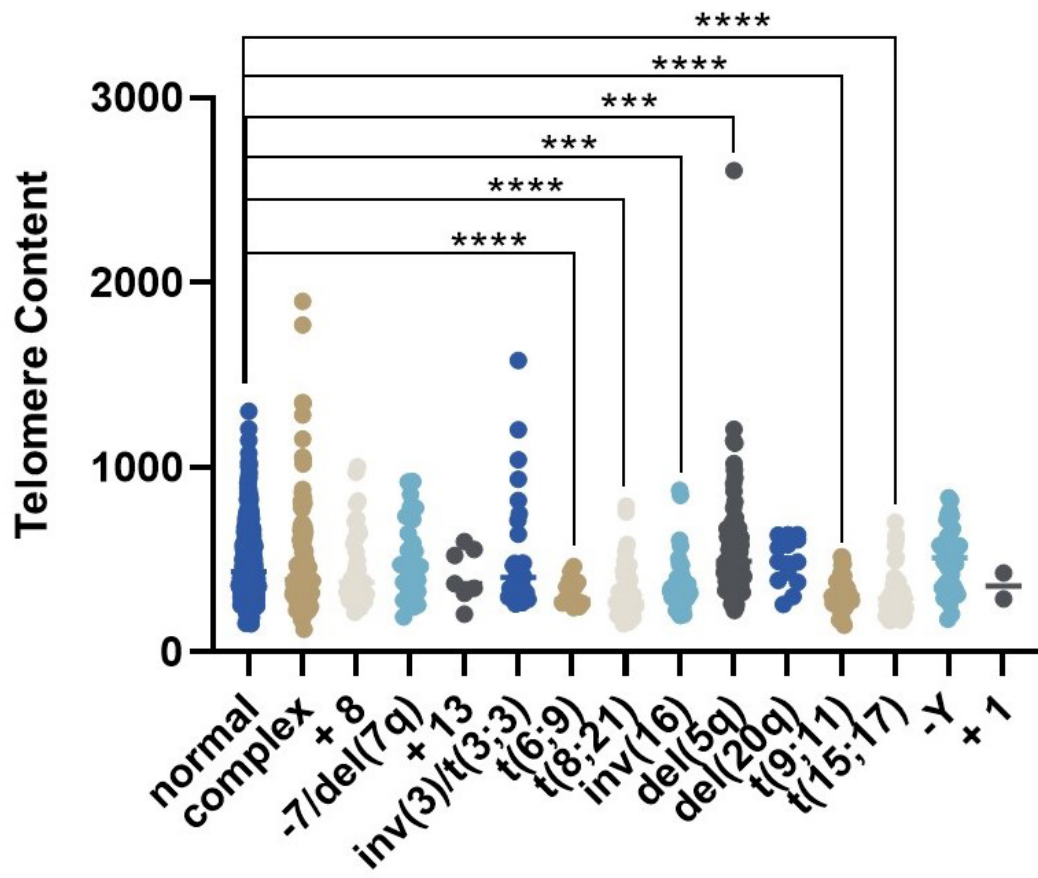
Supplementary figure 3. Correlation of TC with age (A) and blast percentage (B-C).



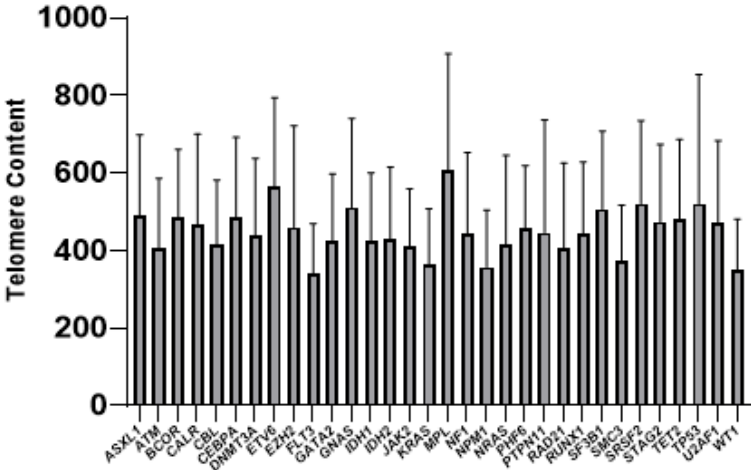
Supplementary figure 4. Telomere content in Acute myeloid leukemia patients grouped according to morphologic FAB classification.



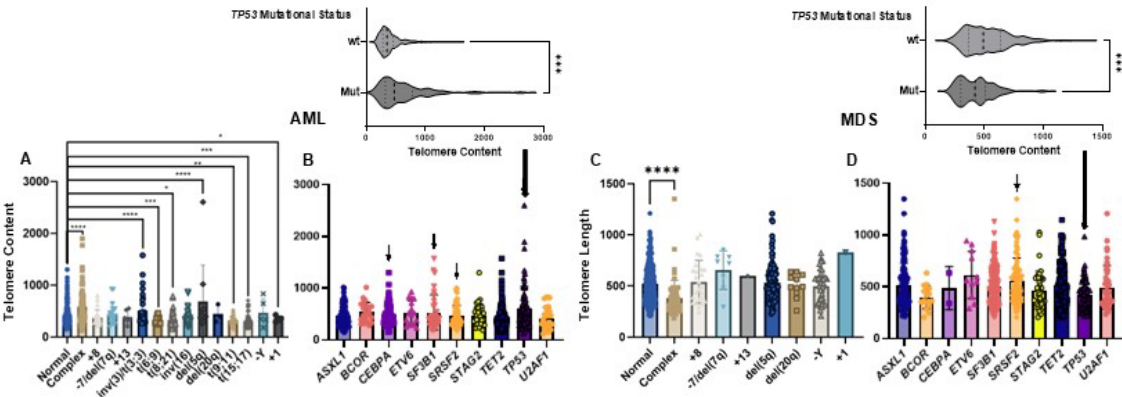
Supplementary figure 5. Telomere content distribution across karyotype anomalies in Myeloid Neoplasia cohort.



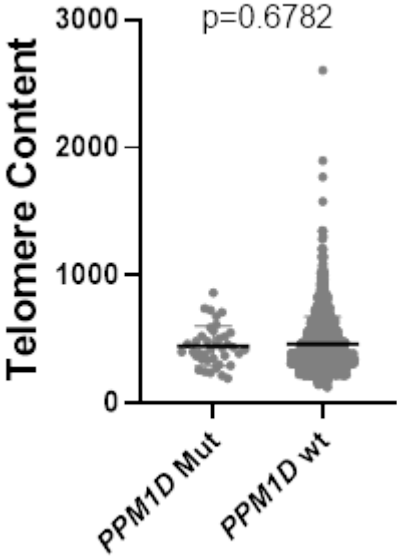
Supplementary figure 6. Telomere content distribution across the mutational landscape of Myeloid Neoplasia cohort.



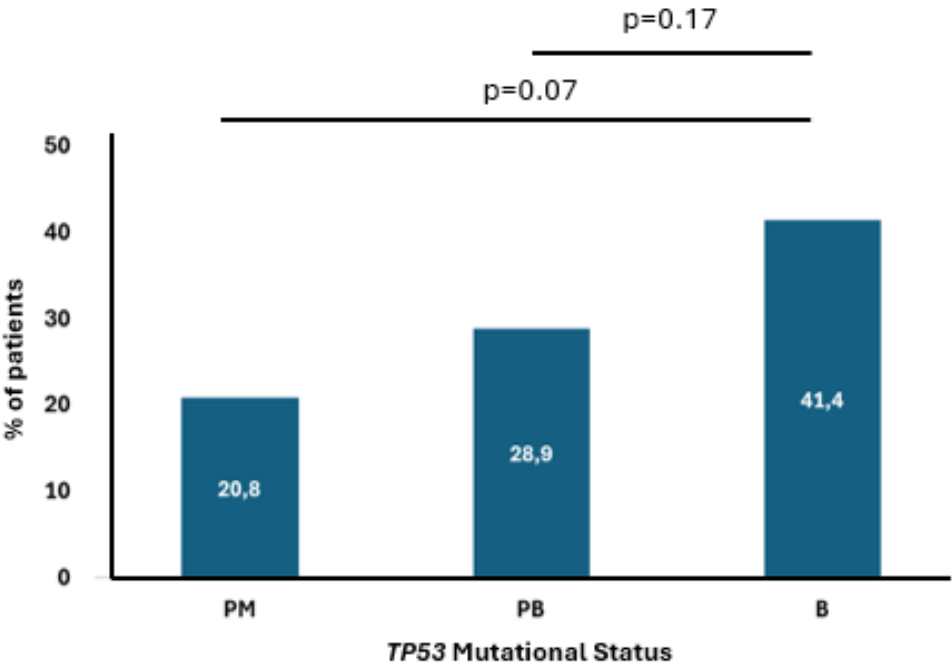
Supplementary figure 7. TC distribution among karyotypic abnormalities and gene mutations in AML (A-B) and MDS (C-D).



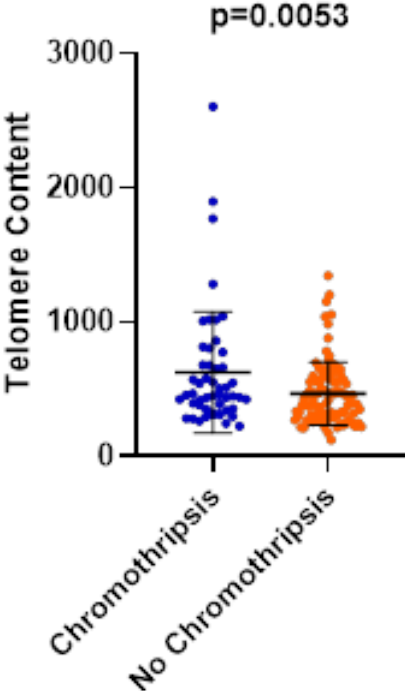
Supplementary figure 8. TC distribution in *PPM1D*- mutated patients vs wt.



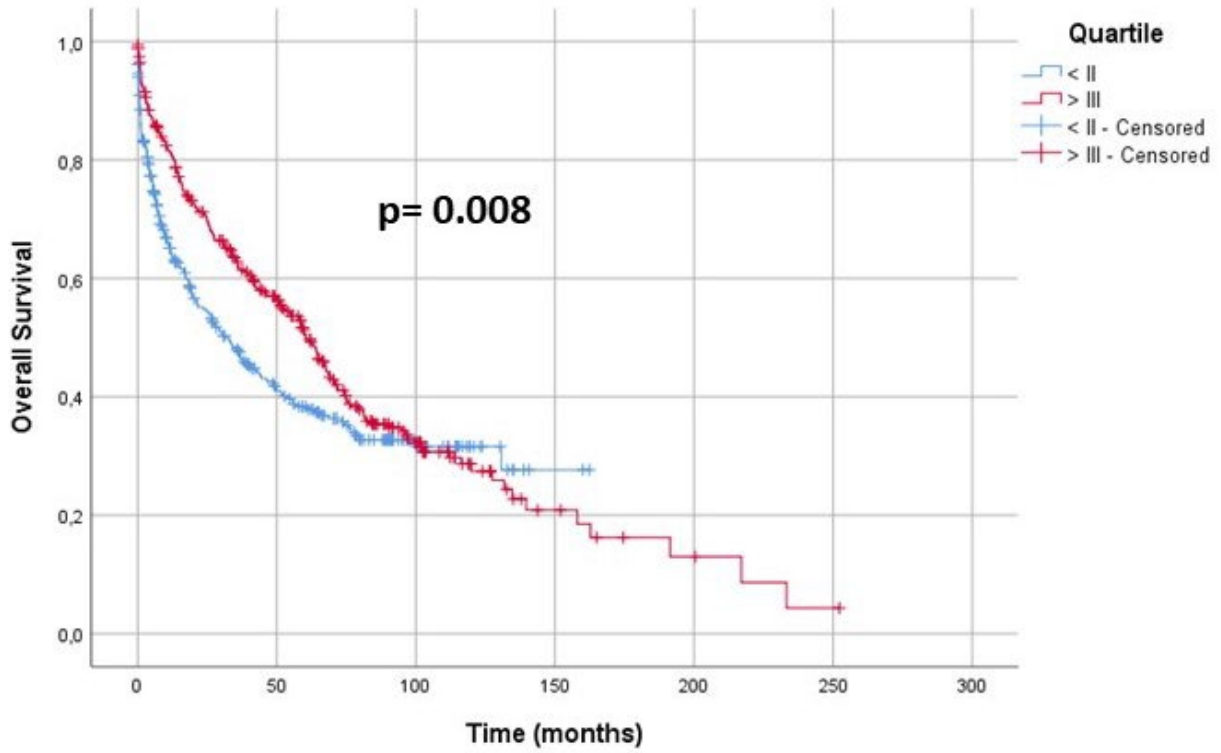
Supplementary Figure 9: Chromothripsis events in TP53-mutated cases according to the size of the clone.



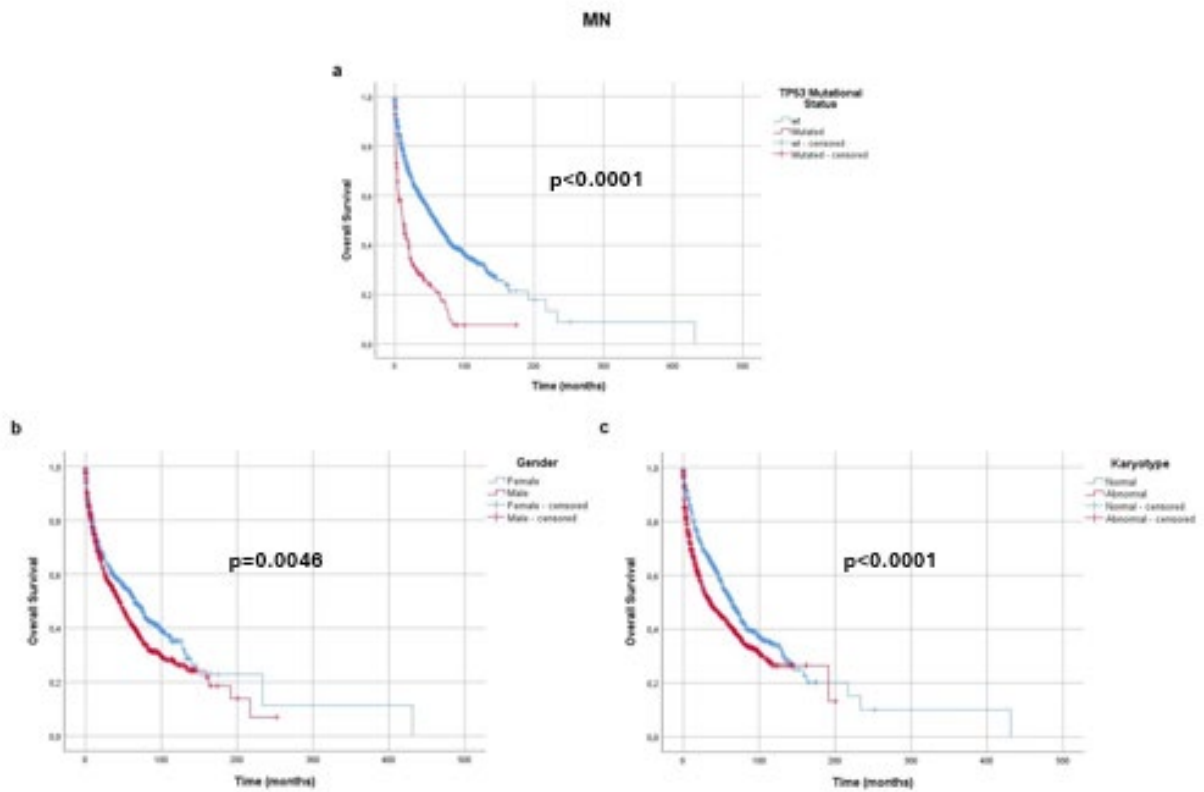
Supplementary Figure 10: TC comparison between TP53-mutated MN with and without chromothripsis events.



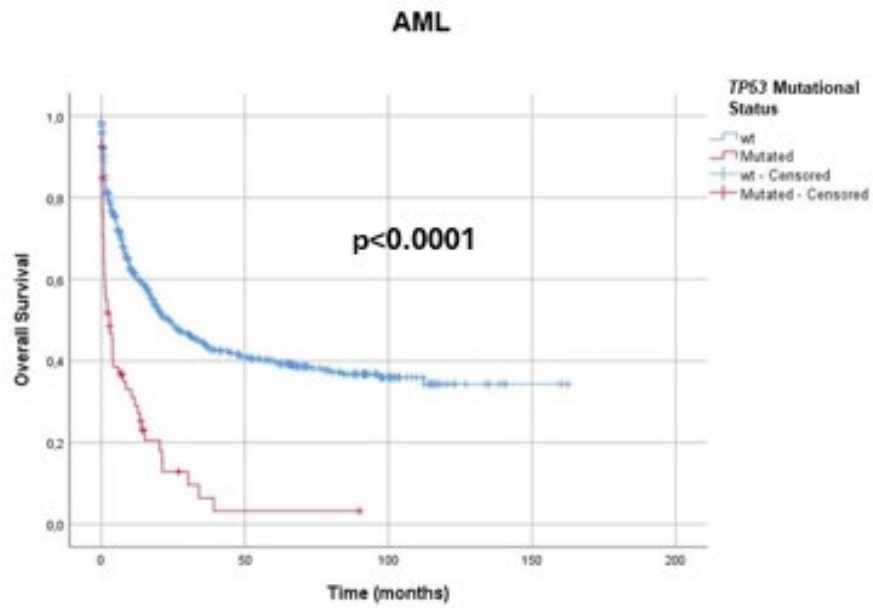
Supplementary figure 11. Kaplan-Meier curves for overall survival in MN patients grouped per telomere content quartile.



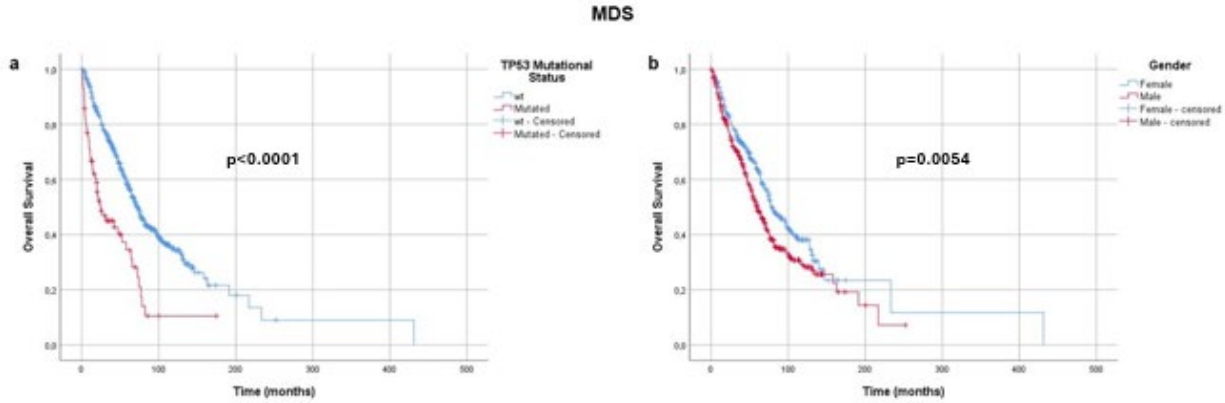
Supplementary figure 12. Kaplan-Meier curve for overall survival in MN patients grouped per *TP53* mutational status (a), gender (b), and karyotype abnormality (c).



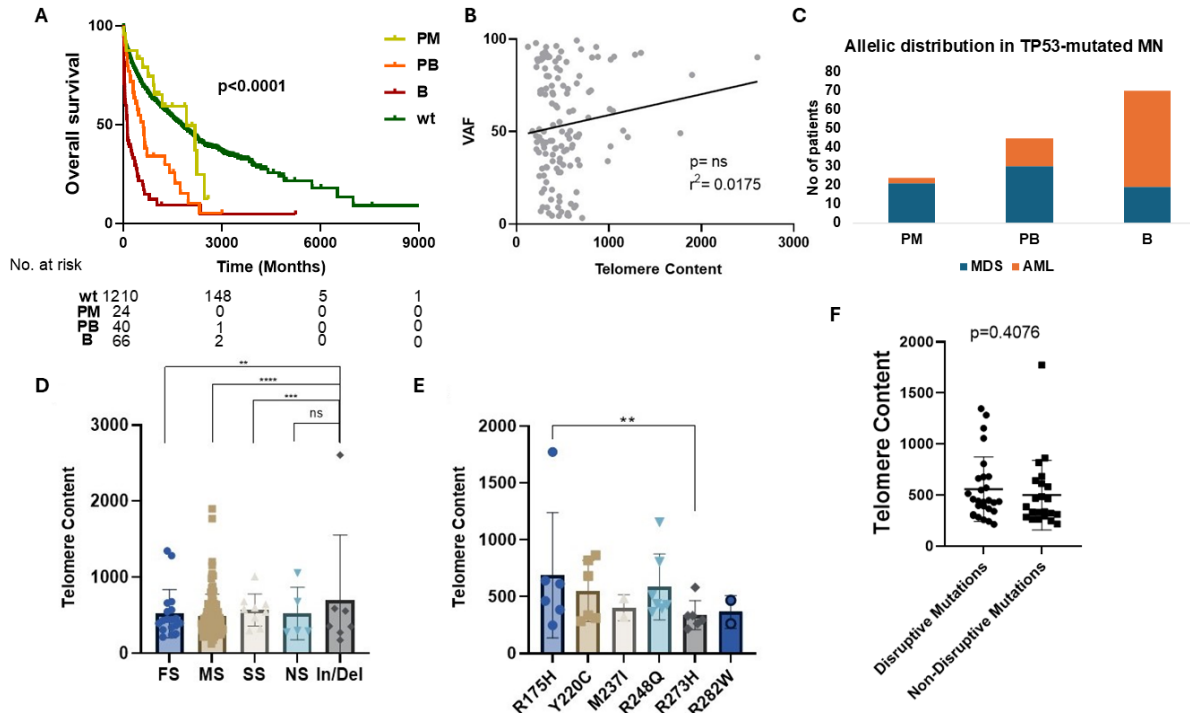
Supplementary figure 13. Kaplan-Meier curves for overall survival in AML patients grouped per *TP53* mutational status.



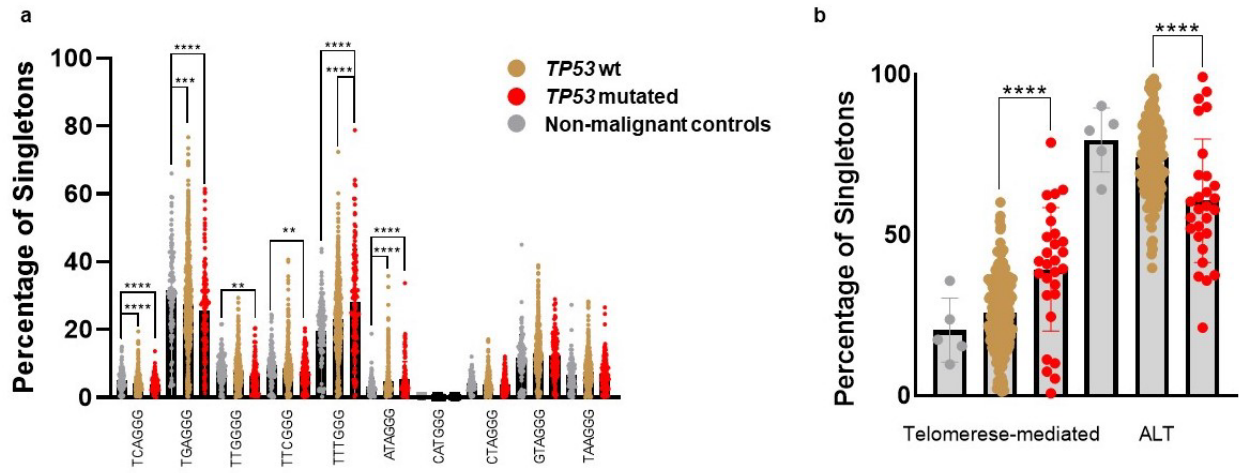
Supplementary figure 14. Kaplan-Meier curves for overall survival in MDS patients grouped per *TP53* mutational status (a) and gender (b).



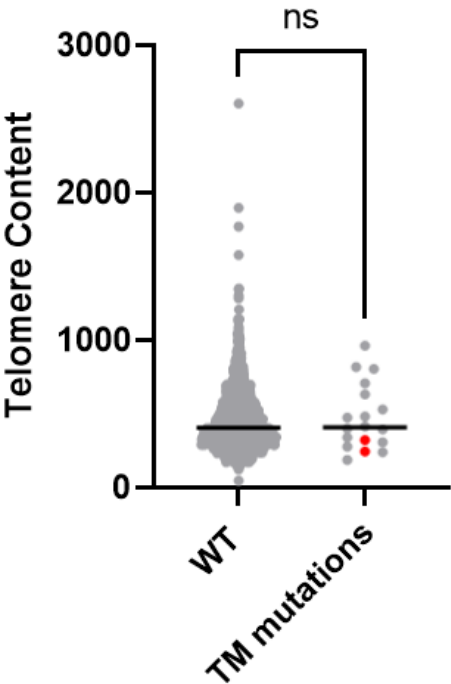
Supplementary figure 15. Telomere content and TP53 mutations features.



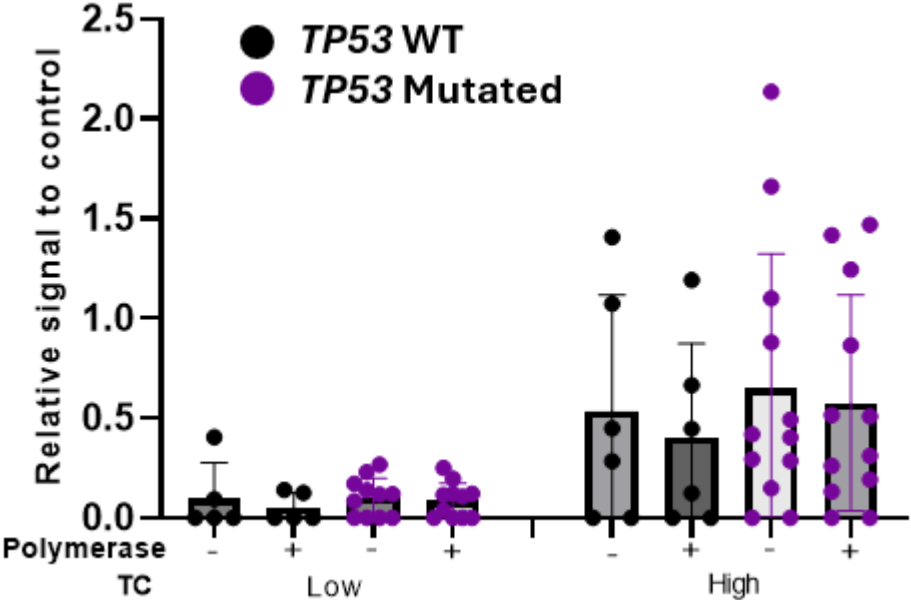
Supplementary figure 16. Singleton analysis.



Supplementary figure 17. Telomere content comparison between patients harboring mutations in telomeres machinery genes (TM) vs WT.



Supplementary figure 18. C-Circle assays for representative samples of different subgroups based on telomere content and *TP53* mutation status.



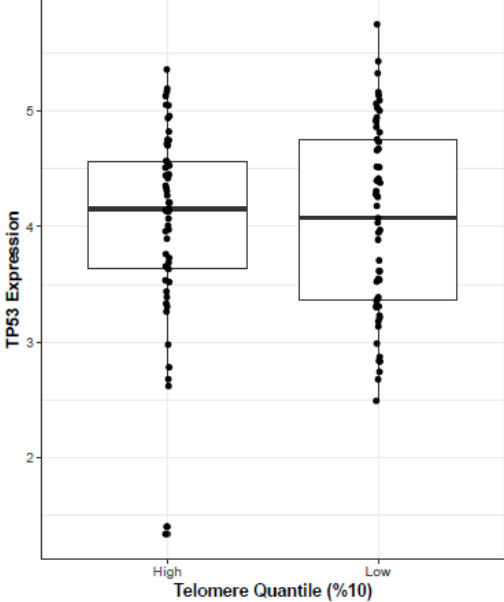
Supplementary figure 19. C-circle analysis-raw data (UPN1-22).



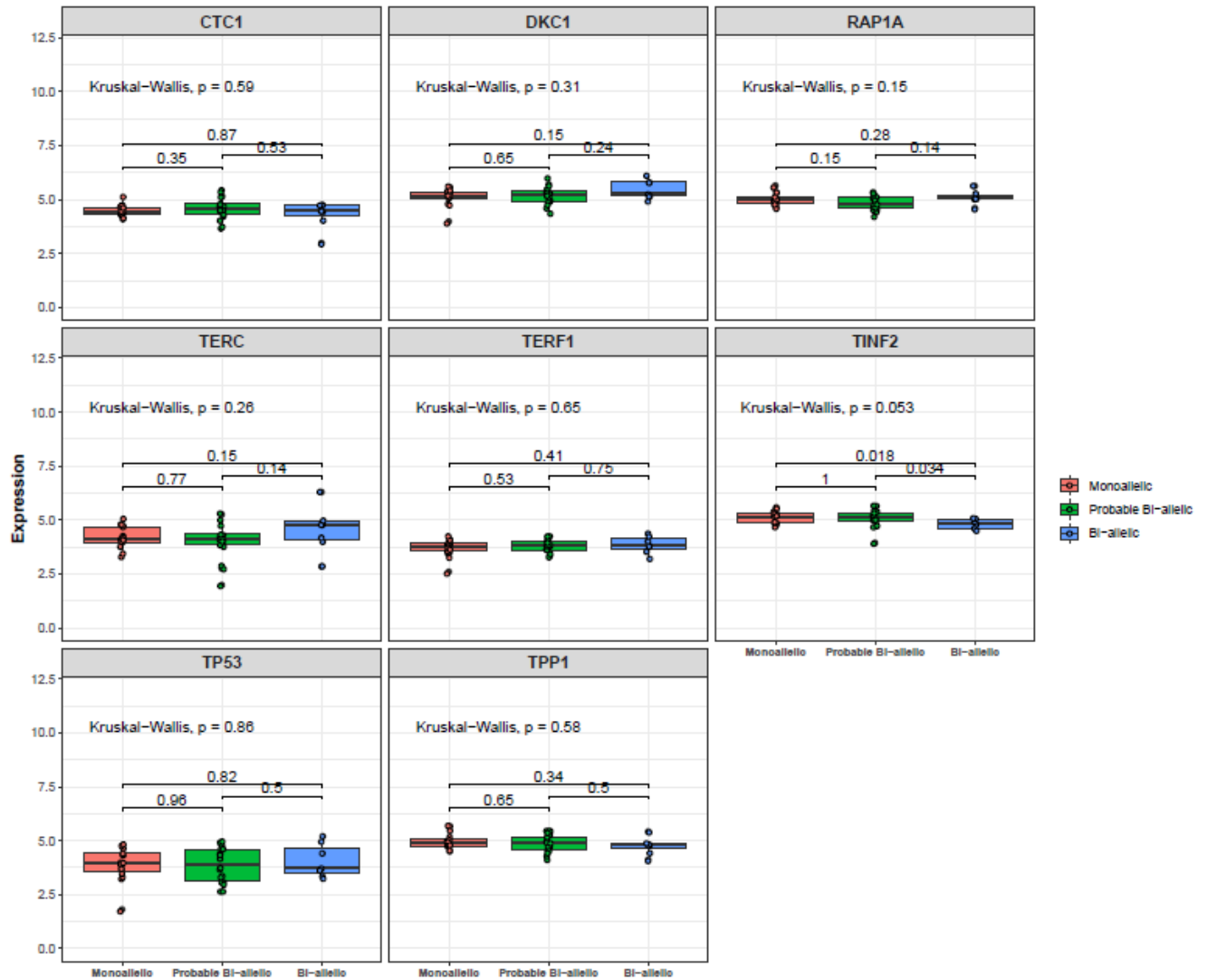
Supplementary figure 20. C-circle analysis-raw data (UPN23-44).



Supplementary figure 21. Correlation between *TP53* expression and telomere content.



Supplementary figure 22. Telomerase machinery gene expression according to *TP53* allelic status.



Legends

Supplementary Table 1. Comparison of TC between non clonal controls and study cohort according to age. AML: acute myeloid leukemia; MDS: myelodysplastic syndrome; MN: Myeloid Neoplasia; TC: Telomere content.

Supplementary table 2. Telomere content and karyotype features in MN population. MN: Myeloid Neoplasia. TC: Telomere content.

Supplementary Table 3. Telomere content and gene mutations in MN cohort. The asterisks represent the significant TC differences between genetic lesions and overall MN cohort. MN: Myeloid Neoplasia. TC: Telomere content.

Supplementary Table 4. Multiple regression analysis for Telomere content including *TP53* mutation. AML: acute myeloid leukemia; MDS: myelodysplastic syndrome.

Supplementary Table 5. Multiple regression analysis for Telomere content accounting for CK. CK: complex karyotype.

Supplementary table 6. Multiple regression analysis for Telomere content, including somatic mutations and karyotype abnormalities correlating with TC and potential biases due to chromothripsis events.

Supplementary table 7. Multivariate analysis for overall survival in MN patients. MN: Myeloid Neoplasia

Supplementary table 8. Multivariate analysis for overall survival in AML patients. AML: acute myeloid leukemia.

Supplementary table 9. Multivariate analysis for overall survival in MDS patients. MDS: Myelodysplastic syndrome.

Supplementary table 10. List of genes involved in telomeres machinery screened.

Supplementary table 11. List of variants identified in MN patients' population.

€Pathogenicity of this variant was assessed by in silico prediction.

“Variant reported by Vanderver et al and Matteucci et al. in hematologic and non-hematologic cancers.^{3,4}

LB, likely benign; LP, likely pathogenic; MN: myeloid neoplasia; P, pathogenic; VAF, variant allelic frequency; VUS, variant of unknown significance; wt: wild type.

Supplementary table 12. Patients included in C-Circle analysis. The table shows the samples of representative subjects, with relative *TP53* mutational status, TL and telomere classification, on which the C-Circle analysis was performed. UPN 18-22 and 40-44 were healthy subjects (HS). TL: telomere length.

Supplementary table 13. Placement of samples in the gel (UPN1-22). See supplementary figure 19.

Supplementary table 14. Numeric quantification of C-Circle analysis results (UPN1-22). SKNBE2 was used as negative control. CHLA90 was used as positive control.

Supplementary table 15. Numeric quantification of C-Circle analysis results normalized to CHLA-90 positive control (UPN1-22).

Supplementary table 16. Placement of samples in the gel (UPN23-44). See supplementary figure 20.

Supplementary table 17. Numeric quantification of C-Circle analysis results (UPN23-44). SKNBE2 was used as negative control. CHLA90 was used as positive control.

Supplementary table 18. Numeric quantification of C-Circle analysis results normalized to CHLA-90 positive control (UPN23-44).

Supplementary figure 1. Study design. To address the study of telomere content in myeloid neoplasia, we relied on whole genome sequencing, to analyze telomere length, clinical data, to establish correlations with disease features and prognosis, RNA sequencing, to assess gene expression differences among subgroups of patients, and C-Circle assay, to detect alternative mechanism of telomere elongation. Non- malignant non-clonal controls included persistent polyclonal B-cell lymphocytosis (PPBL) patients and healthy subjects (HS). Non-malignant clonal controls included aplastic anemia (AA) and paroxysmal nocturnal hemoglobinuria (PNH) patients.

Supplementary figure 2. Impact of aneuploidy in TC. The plots show the correlation between TC and TC adjusted according to type and allele frequency of aneuploidies in patients harboring abnormal karyotype (A), complex karyotype (B), del7/7q (C), +8 (D), del(Y) (E), +1 (F), +13 (G). TC: telomere content.

Supplementary figure 3. Correlation of TC with age (A) and blast percentage (B-C). AML: acute myeloid leukemia; MDS: myelodysplastic syndrome; MN: myeloid neoplasia.

Supplementary figure 4. Telomere content in Acute myeloid leukemia patients grouped according to morphologic FAB classification. The asterisks represent the significant TC differences between M6 and other subtypes. ns: not significant. *: $p < 0.05$; **: $p < 0.01$; ***: $p < 0.001$. TC: Telomere content.

Supplementary figure 5. Telomere content distribution across karyotype anomalies in Myeloid Neoplasia cohort. Asterisks represent significant correlations *: $p < 0.05$; **: $p < 0.01$; ***: $p < 0.001$.

Supplementary figure 6. Telomere content distribution across the mutational landscape of Myeloid Neoplasia cohort. Figure for representative purpose only. Due to overlap among mutations the analysis of the relation between TC and somatic mutations relied on multivariate analysis as explained in the main manuscript.

TC: Telomere content.

Supplementary figure 7. TC distribution among karyotypic abnormalities and gene mutations in AML (A-B) and MDS (C-D). For a better visualization only the somatic lesions with

higher TC and detected in at least 1% of MN population were shown. Upper panels focus on TC comparison between *TP53* mutant vs wt.

Asterisks represent significant correlations. ***: $p < 0.001$. Arrows refer to genes significantly correlated with higher TC when compared to the remaining MN population (For a comprehensive landscape of TC across somatic mutations refer to **supplementary table 3**). AML: acute myeloid leukemia; MDS: myelodysplastic syndrome; TC: telomere content; wt: wild type.

Supplementary figure 8. TC distribution in *PPM1D*- mutated patients vs wt.

MN: Myeloid neoplasia; WT: wild type

Supplementary Figure 9: Chromothripsis events in *TP53*-mutated cases according to the size of the clone.

B: biallelic; PM: probably monoallelic; PB: probably biallelic.

Supplementary Figure 10: TC comparison between *TP53*-mutated MN with and without chromothripsis events.

MN: Myeloid neoplasia; TC: Telomere Content.

Supplementary figure 11. Kaplan-Meier curves for overall survival in MN patients grouped per telomere content quartile. In the picture are represented the survival curves of patients below the first (311.4535, blue curve, 358 patients) and over the third and quartile (566.6146, red curve, 358 patients). Log rank test was used to compare the populations.

Supplementary figure 12. Kaplan-Meier curve for overall survival in MN patients grouped per *TP53* mutational status (a), gender (b), and karyotype abnormality (c). The variables shown were found to be independent predictors of overall survival in the multivariate analysis (see supplementary table 4). MN: Myeloid Neoplasia.

Supplementary figure 13. Kaplan-Meier curves for overall survival in AML patients grouped per *TP53* mutational status. This variable was found to be an independent predictor of overall survival in the multivariate analysis (see supplementary table 5). AML: acute myeloid leukemia

Supplementary figure 14. Kaplan-Meier curves for overall survival in MDS patients grouped per *TP53* mutational status (a) and gender (b). The variables shown were found to be independent predictors of overall survival in the multivariate analysis (see supplementary table 6). MDS: Myelodysplastic syndrome

Supplementary figure 15. Telomere content and *TP53* mutations features. A: Survival of patients according to *TP53* mutational status. **B:** Correlation between telomere content and VAF. **C:** Distribution of *TP53*-mutated MN phenotype according to allelic status. **D:** Correlation between telomere content and type of mutation (FS: frameshift; MS: missense; SS: splice-site; NS: non-sense; In/Del: insertion/deletion), amino acid change (**E**) and functional type of mutation (**F**).

Asterisks represent significant correlations. ns: not significant. *: $p < 0.05$; **: $p < 0.01$; ***: $p < 0.001$.

AML: acute myeloid leukemia, B: biallelic, MDS: myelodysplastic syndrome, MN: myeloid neoplasia, PB: probably biallelic, PM: probably monoallelic, wt: wild type.

Supplementary figure 16. Singleton analysis. **a** Percentage of singletons in *TP53* wt MN (yellow dots), *TP53* mutated MN and non-malignant controls (grey dots). **b** Singletons grouped by telomerase-mediated elongation (TTTGGG) and alternative lengthening one (ALT, the remaining singletons). Asterisks represent significant correlations. MN: Myeloid Neoplasia; wt: wild type. *: $p < 0.05$; **: $p < 0.01$; ***: $p < 0.001$.

Supplementary figure 17. Telomere content comparison between patients harboring mutations in telomeres machinery genes (TM) vs WT. The lists of the TM genes screened and identified are shown in **supplementary table 8 and 9**. The red dots represent *TP53*-mutated MNs.

MN: myeloid neoplasia; wt: wild type.

Supplementary figure 18. C-Circle assays for representative samples of different subgroups based on telomere content and *TP53* mutation status.

TC: telomere content; wt: wild type.

Supplementary figure 19. C-circle analysis-raw data (UPN1-22). See supplementary table 13 for placement of the samples.

Supplementary figure 20. C-circle analysis-raw data (UPN23-44). See supplementary table 16 for placement of the samples.

Supplementary figure 21. Correlation between *TP53* expression and telomere content.

Supplementary figure 22. Telomerase machinery gene expression according to *TP53* allelic status.

References

1. Cortés-Ciriano, I. *et al.* Comprehensive analysis of chromothripsis in 2,658 human cancers using whole-genome sequencing. *Nat. Genet.* **52**, 331–341 (2020).
2. Höllein, A. *et al.* The combination of WGS and RNA-Seq is superior to conventional diagnostic tests in multiple myeloma: Ready for prime time? *Cancer Genet.* **242**, 15–24 (2020).
3. Vanderver, A. *et al.* Whole exome sequencing in patients with white matter abnormalities. *Ann. Neurol.* **79**, 1031–1037 (2016).
4. Matteucci, C. *et al.* TERT Gene Promoter Mutations In Myelodysplastic Syndromes (MDS). *Blood* **122**, 1570 (2013).